# DEVELOPMENT OF ACTIVE FLOW CONTROL MIXED-FLOW TURBINE ON EDDY-CURRENT DYNAMOMETER FOR AUTOMOTIVE TURBOCHARGER APPLICATION

**Apostolos Pesiridis, Srithar Rajoo, Shinri Szymko and Ricardo Martinez-Botas***
**Department of Mechanical Engineering**
**Imperial College London**
**SW7 2AZ Exhibition Road, London**

## ABSTRACT

The increase in particle emissions restrictions in recent years coupled with improvements in such key automotive engine performance areas as low-end torque, increased boost and the elimination of turbolag now required, has led to conventional Variable Geometry Turbochargers (VGTs) to become quite popular in matching turbine inlet geometry to the characteristics of the exhaust gas stream throughout the engine operating range. However, over all these years of turbocharger development the fundamental issue of the less than ideal combination of a reciprocating engine providing energy to drive a rotodynamic machine such as a turbocharger turbine has not been addressed satisfactorily. This paper, therefore, introduces a new concept in turbocharger development, namely, that of active turbocharger flow control. It demonstrates the application of an active flow control device (nozzle) at the inlet to the turbine rotor to help harness the energy contained as a result of the pulsating characteristics of the incoming flow. In the Active Control Turbocharger (ACT), therefore, the nozzle (in this case a sliding vane) is able to alter the inlet area at the throat of the turbine inlet casing (volute) in phase and at the same frequency as that of the incoming exhaust stream pulses. Actuated by a high speed electrodynamic shaker the nozzle can adapt according to the engine exhaust gas pulse pressure variation, thus taking advantage of the lower energy levels existent before and after each pulse pressure peak, which the current systems do not take advantage of. Thus, ACT makes better use of the exhaust gas energy of the engine than a conventional VGT. The experimental work concentrates on the potential gain in turbine expansion ratio and eventual power output as well as the corresponding efficiency trace and nozzle area schedule. Exploration of the full turbine range was made possible by the use of a new eddy-current dynamometer, also, presented here. Early simulation work has, already, provided encouraging results with a theoretical potential gain in terms of cycle expansion ratio and actual power output of approximately 9% and 29%, respectively at typical engine operating points (40Hz or

equivalent to 1600 engine rpm). Direct comparisons between VGT and ACT operation are also provided, at selected, typical, laboratory-simulated engine operating conditions, showing the benefits arising from the use of this innovative technology.

## NOMENCLATURE

| | |
|---|---|
| U | blade tip speed |
| $\dot{m}$ | mass flow rate |
| FGT | Fixed Geometry Turbocharger |
| VGT | Variable Geometry Turbocharger |
| ACT | Active Control Turbocharger |
| Cp | specific heat at constant pressure |
| C | gas inlet velocity |
| $\Delta\vartheta_{ACT}$ | Nozzle amplitude in ACT mode |
| $\vartheta_{null}$ | Normalised open throat area when nozzle is at null point for ACT testing |
| $\vartheta_{VGT}$ | Normalised open throat area in VGT mode |
| ER | turbine expansion ratio |
| P | pressure |
| T | temperature |
| Cp | specific heat at constant pressure |
| MFP | mass flow parameter $MFP = \dfrac{\dot{m}\sqrt{T_0}}{P_0}$ |
| MFT | Mixed Flow Turbine |
| $\dfrac{U_{inlet}}{V_{is}}$ | velocity ratio $\dfrac{U_{inlet}}{V_{is}} = \dfrac{U_1}{\sqrt{\left[2C_P T_{01}\left[1-\left(\dfrac{P_2}{P_{01}}\right)^{(\gamma-1)/\gamma}\right]\right]}}$ |
| $\eta_{t-s}$ | total to static efficiency |

**Subscripts**

| | |
|---|---|
| is | isentropic |
| act | actual |
| 0 | total/stagnation |
| 2 | pulse generator |
| 3 | turbine inlet |
| 4 | turbine exit |

## 1 INTRODUCTION

Automotive turbochargers almost in their entirety are equipped with radial turbines, due to the efficiency superiority of radial designs when compared to other turbine types relative to a given, small size. But radial turbines are limited in their potential, due to their radial leading edge. A mixed flow turbine differs from a radial turbine in that the

leading edge is swept radially downward, as opposed to the zero blade angle of the radial turbine. Research has shown a substantial amount of exhaust gas energy to be available at velocity ratios of less than 0.7 (1) – the point of highest energy recovery for a radial turbine. For a non-zero blade angle the velocity ratio and thus the peak efficiency point moves to a lower velocity ratio, which means a higher pressure ratio. Shifting the peak efficiency point to a higher pressure ratio is advantageous in a turbocharger application, which is subjected to pulsating flows from the reciprocating engine, where the greater energy of the flow is contained at high pressures (2).

On the other hand, the benefits accrued by the use of variable geometry devices for exhaust gas flow control to the turbine are well known and include improved transient response, fuel economy and more importantly reduced emissions in the face of ever stringent emissions regulations. VGTs are becoming increasing popular in recent years and are standard production equipment or standard options after several years of struggling with reliability problems.

Given the extensive research work already carried out by the turbocharger research group at Imperial College on Mixed Flow Turbines (MFTs) on fixed geometry turbochargers (FGTs) and the promising results yielded so far it was decided to expand the scope by studying a novel variable geometry turbocharger capable of actively controlling the flow into the turbine, in combination with the present MFT installed. This Active (flow) Control Turbocharger (ACT) can be run in both ACT mode as well as conventional Variable Geometry Turbocharger (VGT) mode.

A fundamental issue that has so far not been addressed satisfactorily, however, is the less than ideal combination of a reciprocating engine providing energy to drive a rotodynamic machine such as a turbocharger turbine. Yet even with the advent of VGTs this mismatch is not eliminated, since a VGT responds to operating point changes only, i.e., for fixed operating conditions the nozzle setting on a VGT assumes one non-changing, optimal condition. However, regardless of the engine operating point, the inlet conditions to the turbocharger still include a highly pulsating flow field with widely varying pressure and mass flow rate levels. Hence, the energy levels contained within that flow field can still effectively be harnessed, by constantly altering the effective throat area to the turbine by means of a fast-response nozzle.

The aim of this project, therefore, is to introduce the application of an active flow control device (nozzle) at the inlet to the turbine rotor to help harness the energy contained as a result of the pulsating characteristics of the incoming flow. The Active Control Turbocharger (ACT) is a special type of VGT, where the nozzle (in this case a sliding vane) is able to alter the inlet area at the throat of the turbine inlet casing (volute) in phase and at the same frequency as that of the incoming exhaust stream pulses. For this purpose it is actuated by a suitable electrodynamic shaker - in turn supplied by a powerful amplifier - capable of meeting the frequency and displacement requirements of this intensive and continuous operation.

## 2 LITERATURE REVIEW

## 2.1 Mixed flow turbines

The concept of mixed-turbine was initially studied for the first time in the early 1950s for aerospace application. By the early 1970's the possibility of using mixed-flow turbine was introduced to overcome the problems associated with a radial turbine. For the past three decades research has concentrated in proving the superiority of the mixed flow turbine in terms of lower velocity ratio operation and higher mass flow rate (4, 5, 6, 7). Apart from these, the mixed flow turbine has, also, been developed as part of engine development in recognition of its advantages (8, 9, 10, 11). Despite some disadvantages such as larger weight by comparison to a radial turbine, giving rise to dynamic problems as well as a more complicated to design for stress reduction (12), the mixed flow turbine is possibly the wisest option to replace a radial turbine with in order to keep up to the ever increasing engine requirements.

## 2.2 Variable geometry turbocharging

Although the concept of VGT is not entirely new (the first examples appearing in the early 1960's) their development did not gain impetus until fairly recently. Up until the early 1980's VGTs were rarely used except on gas turbine plants and experimental turbochargers. The common problems encountered with VGT were reliability (for long periods of time while exposed to high temperature and corrosive exhaust gases), complexity because of the VGT actuation mechanism and control system, and subsequent, high cost (14). However, recent research has tended to provide acceptable solutions to most of these problems and today, VGTs have already had a significant impact in the design of small diesel engines.

Many VGT devices have been tested over the years such as movable volute tongue, pivoting nozzle vanes, moveable sidewall and sliding nozzle. Comparison of the performance of the various VGT types has shown that pivoting vanes and sliding nozzles afford higher performance and better reliability and are the designs of choice for turbochargers produced today (15, 16, 17). The current project utilised a lightweight sliding nozzle for VGT and ACT testing (Fig.4).

Most available published work on VGTs is still based on steady-state data. Exceptions have used averaged pulsating data in combination with VGT, from which empirical factors are derived to compare steady and unsteady data (18). The present experimental facility, however, offers the ability for both steady and pulsating flow testing of the VGT, equipped with a mixed flow turbine for the first time. The scope of steady state testing of a VGT is to develop ACT operating schedules. From past research, however, it has been shown that the turbine performance during pulsating flow departs substantially from the quasi-steady assumption (6, 7). Thus unsteady-state VGT testing is required in order to define alternate and perhaps more optimal ACT operating schedules and more importantly to provide a basis to compare against ACT data since unsteady tests provide a closer match to real life engine operation..

# 3 EXPERIMENTAL TEST FACILITY

The turbocharger aerodynamic test facility is a simulated reciprocating engine test bed for turbocharger testing. Engine pulsations are simulated by pulse generator plate cut-outs. As there is no real engine and warm air not hot exhaust gas is the flowing medium, equivalent conditions are used, which are summarised in Table 1:

**Table 1 – Design Conditions (3)**

| Parameter | Design Condition | Equivalent Design Condition | Units |
|---|---|---|---|
| Pressure Ratio | 2.91 | 2.91 | -- |
| Inlet Temperature | 923 | 344 | K |
| Mass Flow Rate | 0.414 | 0.678 | kg/s |
| Rotational Speed | 98,000 | 60,000 | rpm |

Compressors provide compressed air instead of hot exhaust gas to simulate flow into the turbocharger and heaters warm the air up to the required inlet conditions.

The present facility introduces three new features to advance the research already carried out by this group previously on MFTs. In addition to new instrumentation, a permanent magnet, eddy current dynamometer is now used in place of the previous compressor, as well as a novel Active (flow) Control Turbocharger.

### 3.1 Instrumentation

The instrumentation for control, monitoring, data logging and data post processing has been modified and upgraded to an automated system through the use of two computers, which now undertake the entire experimental task.

One computer handles all normal control functions such as air flow and pulse generator frequency regulation, as well as steady-state monitoring and data logging through the use of Fieldpoint distributed, network I/O modules to the static pressure, temperature and frequency counters. The second computer is used for high speed data acquisition as well as to control the electrodynamic shaker which actuates the ACT. For this task two high-speed PCI boards are utilised. In addition, an external function waveform generator is used as part of the ACT control system.

### 3.2 Eddy current dynamometer

#### 3.2.1 Introduction

Dynamometers are used to measure the power, from which the efficiency of turbocharger turbines can be estimated. The dynamometer requirement for small turbomachines such as turbocharger turbines need to operate at very high speeds, typically 100,000~200,000 rpm. The rotational part of the dynamometer must be light in weight and have a small polar inertia; otherwise the bearing system on the turbocharger will fail. Because of the wide operating conditions of the turbocharger turbines, the power range requirement of the dynamometer is large. When engine simulations are carried out with quasi-steady methods to model the pulsating flow conditions in the engine manifold and its turbocharger, a turbine map with very wide operating conditions is required. A possible method to obtain such a map is by using the compressor of the turbocharger to load the turbine, unfortunately the range of data using this method would be insufficient given the

surge and choke margins of the compressor. An eddy current dynamometer used as the loading device thus offers a much broader range of testing without the associated aerodynamic limitations of the compressor it now replaces.

Due to the pulsating inflow condition in a turbocharger turbine, the instantaneous performance does not follow the steady characteristic curve (7); but rather a hysteresis loop that encircles the steady result is obtained. To measure the instantaneous torque or power of the turbines, it is essential to know the polar inertia of the rotational assembly of the dynamometer; hence an eddy-current based dynamometer is superior over the hydraulic dynamometer. Furthermore the light nature of the dynamometer used ensures that the instantaneous performance of the turbine can be measured without appreciable damping effects.

In the past, permanent magnet technology could not meet the requirements of turbocharger dynamometers because of the high demagnetisation field generated by the eddy currents. With the advent of rare-earth magnets such as Neodymium-iron-boron magnets with their high resistance to demagnetisation, their use has become practical in dynamometers.

### 3.2.1 Description

If a conducting disk is exposed to a changing magnetic field caused by the relative motion of a permanent magnet translating above its surface, eddy-currents are induced within the conductor. These eddy-currents generate their own magnetic field that will oppose the source field; the magnet will experience reactionary forces. These forces manifest themselves as both a repulsion and a retardation force. It is this latter force that is utilized by the dynamometer; the retardation force multiplied by the relative velocity yields the power absorbed by the dynamometer. This power is also equal to the heat that must be removed from the stators in order to maintain a stable system. Figure 2 shows a simplified model of the dynamometer principle.

The dynamometer utilises the principle of eddy-current braking by incorporating Neodymium-Iron-Boron magnets in a spider creating a low inertia axial flux rotor.

The rotor developed incorporates 14 ground Neodymium-Iron-Boron magnets of 10mm depth. These were positioned with alternate polarity in an aluminium spider to create a 14-Pole axial flux rotor. This rotor spins co-axially to a set of stationary water-cooled conducting plates known as the stators, which are located on either side of the rotor (Fig. 3). A carbon-fibre ring was used to externally support the magnets giving an overall diameter of 80mm, whilst a central steel spigot was used to create the required interference fit in order to secure the magnets in place. Water-cooled stators were placed on either side of the rotor. This allows the dissipation of a greater amount of power whilst alleviating the problem of the axial thrust created by the eddy-currents. The movement of the stators was remotely controlled in a stepper motor system. By altering the gap between the stators and the rotor the power that the dynamometer absorbs can also be altered. This type of set-up requires very few components and gives rise to a mechanically simple, cheap and compact design.

The stators were cooled with approximately 35 litres a minute of untreated water, which flows radially against its back surface. To stop interference with the torque measurement the coolant enters and exits the rig axially and hence does not contribute to the measured

torque. The torque was measured directly by mounting the whole system freely on a pair of gimble bearings. A lever arm connected to the free-floating components is reacted against a load transducer and this gives the torque produced by the turbine (minus the resistance torque of the gimble bearings).

### 3.2 Active control turbocharger

#### 3.2.1 Design

The main ACT components can be seen in Fig. 4 and 5. A nozzleless Holset H3B turbocharger turbine was modified to accept a nozzle for VGT testing. Due to the very small space available a very thin (1.5mm thickness) section, tubular form, sliding nozzle was designed. Two embedded attachment points towards the back end (away from the volute) are used to mount the nozzle on to its actuating arm (yoke) via two small bearing pads, which fit between the nozzle and the actuator arm and assist in translating the pivoting movement of the yoke into a linear motion by the nozzle. The nozzle itself is guided towards the throat by an inner guide, which serves both as a bearing surface to the nozzle as well as the exducer section of the turbine. An outer guide houses the entire assembly and at its lower end is shaped into a bracket on which the yoke is attached and can freely pivot about. The entire assembly is held together and attached to the face of the turbine by six long M5 bolts. The throat width to the turbine is 26mm wide and the nozzle can block approximately 22mm off that passage width before reaching the stops.

The materials used for the assembly were 6082-T6 aluminium alloy, for the entire assembly except for the nozzle, providing light weight, with adequate strength to overcome (in the case of the yoke) fatigue, which was the major issue in its operation. At the most severe operation the yoke achieved a safety factor of 10 with respect to the maximum bending stress applied to it at its corners by the bearing pads. The nozzle was of CFRP construction, providing adequate strength against the high pressure air flow used during testing for ultra low weight - low nozzle weight being critical for the whole ACT in achieving good force performance.

A V406 electrodynamic shaker was used to drive the nozzle in ACT mode. The shaker was chosen so as to be able to provide the required force for the frequencies and amplitudes expected during testing (60Hz and 20mm, respectively). Direct coupling of the shaker and nozzle was not possible due to the nozzle being driven from the exhaust side of turbine, thus forcing the shaker to be offset to the side of the exducer. The simplest way to drive the nozzle from this position was with a single-piece, pivoting fork-type actuator arm. This makes the design, simpler, more compact and more importantly allows for far better fatigue endurance with the added advantage of significant vibration damping due to the rocker-arm type operation of the yoke used to drive the nozzle, which largely damps out what would otherwise have been severe vibrations through the turbocharger. The total mass of all moving parts (Part Nos. 2, 3, 4, 8 and 9 in Fig.4(a)) is only 0.241kg, which was important in order to be able to achieve the force performance required for testing, even though it means a penalty in terms of vibration, since at present it is not possible to balance both sides of the yoke, as the top part (nozzle) is significantly lighter to the bottom part that also contains approximately 0.2kg of the moving part of the shaker.

#### 3.2.2 Operation

The electrodynamic shaker is connected to the lower part of the yoke through an adjustable lever (Fig.5) used to set the nozzle restriction ( $\vartheta_{VGT}$ ) in VGT mode or the null point ( $\vartheta_{null}$) in ACT mode. The amplitude, frequency and form of the controlling signal is controlled by a function waveform generator, which sends it to a 100W amplifier as well as to the controlling computer. From the amplifier the signal is routed to the shaker and transformed into motion of the nozzle. Two high speed pressure transducers one immediately downstream of the pulse generator and one immediately upstream on the turbine inlet are used to measure the inlet pressure level $P_1$. By timing the two pressure signals as they arrive at the high speed data acquisition board the time delay measured is used to trigger the shaker by triggering the waveform generator first. Thus, the shaker is always in phase with the inlet pressure signal. An LVDT nozzle position transducer is used for feedback (Fig.8(a)).

For VGT testing $\vartheta_{VGT}$ can be set by adjusting the lever only. For ACT testing, $\vartheta_{null}$ is adjusted manually, while $\Delta\vartheta_{ACT}$ and the shaker frequency are preset on the waveform generator according to the test parameters required. Typical $\vartheta_{VGT}$ test points used during testing have included the following:

**Table 2 – Nozzle VGT settings for the 26mm wide throat area**

| **Nozzle restriction into throat (mm)** | $\vartheta_{VGT}$ |
|---|---|
| 0 | 1 |
| 4 | 0.846 |
| 8 | 0.692 |
| 12 | 0.538 |
| 16 | 0.385 |
| 20 | 0.231 |

## 4 STEADY STATE TEST RESULTS

### 4.1 Dynamometer with fixed geometry turbocharger

The final dynamometer results are shown in Fig.6 (a) and (b) in the form of turbine performance maps and correspond to an equivalent $\vartheta_{VGT}$ setting of 1, i.e., a fully open throat area, even though all tests were carried out on the original turbine volute, which is a fixed geometry turbocharger. Only the 60% equivalent turbine speed data are shown. The range previously available by using a compressor as the loading device typically lied between a velocity ratio of 0.6 and 0.8. It can be seen that, the range of the data obtained with the eddy current dynamometer has been increased by at least three fold, resulting in a much more complete turbine map. Tests previously impossible to carry out, such as high velocity ratio (i.e., very low power) tests, are now available. However, at the maximum velocity ratios, careful and repeated testing is needed as the load cell torque offset error becomes significant and observing the proper experimental technique in acquiring torque data is paramount.

One of project goals, namely, expansion of the available turbine test range and particularly very low power testing, through the development of a new dynamometer has been achieved with the velocity ratio range now spanning a maximum of between 0.35 to 1.1 – this maximum range being achieved at a turbine speed of 29400rpm.

### 4.2 Dynamometer with variable geometry turbocharger

The steady-state VGT results can be seen in Figures 6 and 7. Turbine map plots of efficiency against velocity ratio and MFP versus ER are presented for the three constant speed parameters (50%, 60% and 70% equivalent turbine speeds) however the plots focus on 60%, at which maximum turbocharger efficiency has been reached. The 50% equivalent turbine speed corresponds to approximately 29400rpm, while 70% to 41400rpm.

From the efficiency plots it immediately becomes apparent that there is a large efficiency drop as the throat restriction increases. This was expected as with every VGT mechanism disturbing the flow to the turbine, in the form of stagnating flow on the outside surface of the sliding nozzle as well as increased turbulence off the sharp edged tip of the nozzle. It is significant to notice that for relatively small restrictions (down to 0.692 or even 0.538) the drop in efficiency is typically less than 10%, while it becomes significantly higher at larger restrictions.

On the other hand, from the mass flow parameter against expansion ratio plots, it can be seen that even though, the smaller restrictions do not suffer a significant drop in efficiency they do not produce initially any appreciable increase in expansion ratio, whereas at approximately the same restrictions where the efficiency drop becomes significant the expansion ratio gain becomes more pronounced. Therefore, the effect that the throat restriction has on expansion ratio increase becomes evident.

Unfortunately, due to project constraints it was not possible to match an optimal MFT-oriented nozzle design to the present MFT. Instead, a straight nozzle was used with the MFT rotor as opposed to a downwards inclined nozzle in the radial direction to follow the MFT leading edge angle, thus resulting in interspace diffusion effects causing adverse VGT performance, since the resulting triangular interspace between nozzle and rotor, causes flow diffusion and therefore a decrease of the velocity component, C, hence less actual energy recovered at the turbine itself.

## 5 ACTIVE FLOW CONTROL TURBOCHARGER

### 5.1 Numerical Simulation

The main aim of the numerical simulation was to demonstrate the ability of an ACT to enhance the exhaust gas energy recovery in the turbine, by comparison to a conventional VGT, since outside of the optimum engine/turbocharger matching point the energy recovery suffers significantly.

A standard one dimensional matching calculation was used and is based on a procedure described in literature (14). The main, general assumptions made in this model involve a quasi-steady approach, a high response actuator, inlet and outlet velocities small enough

to neglect difference between static and total values of pressure and temperature and all types of losses at the inlet and exhaust manifold have been neglected.

Due to the nature of the engine-turbocharger match (volume machine combined with a speed machine) the cycle averaged power output of the turbocharger is less than what it could be if the turbine inlet pressure level could be raised instantaneously to its peak pressure instead of fluctuating substantially between atmospheric levels and its peak value. The ideal case, therefore, is for an ACT turbocharger to virtually eliminate exhaust gas pulsation at entry to the turbine so that the turbine inlet pressure at any instant of time is equal to the peak pressure of an equivalent pulse in a standard VGT-equipped turbocharger. This, however, is not possible due to limitations on maximum nozzle displacement, efficiency drop and the fact that at the end of the pulse period the inlet pressure levels are near atmospheric and therefore, it is not possible to increase the inlet pressure significantly at this stage.

An example of the gain afforded by an ACT can be seen in Table 3, where a significant increase in pressure and power levels can be seen by comparison to a conventional turbocharger. It may, also, be observed that this power increase comes at the expense of efficiency, which was expected but this did not have a very detrimental effect on the power recovered.

**Table 3 – Conventional turbocharger comparison with ACT performance (max. nozzle restriction)**

| Parameter | Cycle-averaged VGT data | Equivalent data for ACT |
|---|---|---|
| Inlet pressure (bar) | 1.584 | 1.93 |
| Mass flow rate (kg/s) | 0.2531 | 0.1538 - 0.3498 |
| Turbine speed (rps) | 685.9 | 694.2 |
| Actual Power (W) | 17859 | 26943 |
| Isentropic Power (W) | 24770 | 50471 |

### 5.2 Operating Schedule based on stead-state VGT test results

The ACT test phase will use initially, as a baseline the unsteady-state FGT results although eventually the superiority over equivalent cycle, unsteady-state VGT power results will need to proven.

The purpose of the steady-state VGT tests carried out, was to develop a realistic nozzle ACT schedule (in terms of amplitude and null points) for different operating conditions (turbine speed, dynamometer load and pulse generator frequency). From Fig.6(b) it may be seen that on the initial steep gradient part of the MFP over ER curves, for a constant MFP, (which is what quasi-steadily applies to an ACT nozzle, instantaneously) large nozzle amplitudes are required to achieve modest inlet pressure gains. Above approximately 1.4bar the slope becomes significantly flatter offering much larger gains in terms of pressure. However, at the same time there is a corresponding decrease in efficiency (Fig.6(a)). It is:

$$W_{t,is} = \dot{m}_t Cp_{exh} T_3 [1 - \left( \frac{P_3}{P_4} \right)^{\frac{1-\gamma_{exh}}{\gamma_{exh}}} ]$$

and $W_{t,act} = n_t W_{t,is}$

In the effort to recover more energy out of the exhaust gases, increasing the pressure drop across the turbine is one way of achieving this aim provided, however, the resultant efficiency drop can be held within tolerable limits. Therefore, the disparity between the FGT efficiency and the efficiency at any intermediate nozzle position ( $\Delta\eta_{t-s}$ ) needs to be minimised. From Fig.6(a), minimum efficiency difference occurs only at the ends of the velocity ratio range as at between 0.6 to 0.7 the FGT efficiency reaches its peak, whereas the VGT efficiencies exhibit a flatter curves thus increasing the disparity at the FGT peak efficiency velocity ratio range.

In Fig.7 it may be seen that only at the higher loads and in any case only at significant throat area restrictions (below 50% open for the higher loads) does energy become available for increased recovery. At very low powers (10mm, 7mm and even 5mm dynamometer gaps) a high percentage of energy may be recovered but it is overall too small in quantity when compared to the peak energy levels available at other parts of the pulse. At 5mm gap, some energy may be recovered but in any case at low powers a throat area of 25% open or less is required for any sort of appreciable effect.

In addition ACT operation is also limited by the frequency of the generated pulse. In Fig.8(b) it may be seen that due to actuator dynamic performance the maximum amplitudes are available, only at the lower frequencies (below 30Hz). It, therefore, becomes apparent that the most beneficial area for ACT energy extraction is at inlet pressures above 1.4bar and at velocity ratios higher than 0.6 (or at very low velocity ratios) and at frequencies of less than 30Hz.

A final implication of the present setup is connected to the control schedule that ACT operates on and in particular, the phasing between the different hardware components and the impact this has on performance. At present, the assumption is made that the pressure peaks between an FGT (or VGT) pulse and the ACT pressure trace form need to be in-phase. Fig.8(a) shows with solid lines the pressure at the pulse generator located way upstream of the turbine and the pressure at the turbine inlet. The function waveform generator is activated by the pulse generator pressure and the final waveform is the LVDT nozzle position trace. For simplicity the FWG provides a sinewave to the shaker as the controlling signal. A typical pressure waveform is not a sinewave but was considered similar enough to a sinewave in order for the latter to be selected as the controlling waveform. The location of a second pressure peak at near the end of the pressure pulse is encouraging as it means more energy may be recovered throughout the pulse period rather than at only the higher pressure regions of the pulse.

## 6 CONCLUSION

The aims of the present work were threefold: to prove the new eddy-current dynamometer, to demonstrate the performance of an MFT with a VGT device and highlight the difficulties of matching the two and to present the novel ACT concept and demonstrate its theoretical potential along with early experimental work aiming at optimising the ACT operating schedule.

The new dynamometer has proved successful in obtaining experimentally for the first time, near complete turbine performance maps for engine simulation codes and for CFD validation purposes.

Some initial conclusions could be drawn from applying a VGT operation to a nozzleless FGT equipped with an MFT rotor, in that large throat restrictions are required for appreciable gains in ER but also with significant efficiency losses too. The latter are part of the non optimal design match between the straight nozzle and the inclined MFT leading edge causing interspace losses.

In terms of employing the turbocharger for ACT operation, there does seem to be potential, however, it is hampered by high losses and therefore the energy recovery is not as high as theoretically possible. By focusing at certain parts of the operating envelope (low pulse frequency operation, operation at low or very high powers and large area restrictions) the potential of the present ACT may be demonstrated.

## 7 ACKNOWLEDGEMENTS

The authors would wish to thank the Engineering and Physical Sciences Research Council (E.P.S.R.C) for their financial support, Holset Engineering for their technical support, in particular that provided by N. Sharp, and N. Karamanis for the experimental data.

## 8 REFERENCES

1. Hakeem, I., 1995, **"Steady and unsteady performance of mixed flow turbines for automotive turbochargers",** Ph.D. Thesis, Imperial College of Science, Technology and Medicine, London, England.
2. Palfreyman, D., and Martinez-Botas, R. F., **"Numerical study of the internal flow field characteristics in mixed flow turbines",** Proceedings of ASME TURBO EXPO 2002, ASME GT 2002-30372, 2002.
3. Palfreyman, D., and Martinez-Botas, R. F., **"The pulsating flow field in a mixed flow turbine: An experimental and computational study",** Proceedings of ASME TURBO EXPO 2004, ASME GT 2004-53143, 2004.
4. Baines, N.C., Wallace, F.J. and Whitfield, A. **"Computer Aided Design of Mixed-Flow Turbines for Turbochargers",** Transc. ASME, Vol 101, July 1979, p.p. 440-449
5. Abidat, M., Chen, H., Baines, N.C., **"Design of a Highly Loaded Mixed Flow Turbine"**, Proc. Instn. Mech. Engrs., Vol 206, 1992.
6. Arcoumanis, C., Hakeem, I., Khezzar, L. and Martinez-Botas, R.F. **"Performance of a Mixed Flow Turbocharger Turbine Under Pulsating Flow Conditions",** ASME 95-GT-210, 1995
7. Karamanis, N., Martinez-Botas, R.F. **"Mixed-Flow Turbines for Automotive Turbochargers : Steady and unsteady Performance"** Int. J. Engine Research Vol 3, No.3, IMechE 2002.
8. Yamaguchi, H., Nishiyama, T., Horiai, K. and Kasuya, T. **"High Performance Komatsu KTR150 Turbocharger",** SAE Paper 840019, 1984

9. Ikeya, N., Yamaguchi, H., Mitsubori, K. and Kondoh, N. **"Development of Advanced Model of Turbochargher for Automotive Engines",** SAE Paper 920047, 1992
10. Tsujita, M., Niino, S., Isizuka, T., Kakinai, A. and Sato, A. **"Advanced Fuel Economy in Hino New P11C Turbocharged and Charge-Cooled Heavy Duty Diesel Engine",** SAE Paper 930272, 1993
11. Minegashi, H., Matsushita, H. and Sakakida, M., **"Development of a Small Mixed-Flow Turbine for Automotive Turbochargers"**, ASME 95-GT-53, 1995.
12. Rodgers, C., **"Review of Mixed Flow And Radial Turbine Options",** AIAA Paper 90-2414, 1990
13. Baines, N.C., "**Radial and Mixed Flow Turbines Options for High Boost Turbocharger"**, 7th Int. Conference on Turbocharger and Turbocharging, 2002.
14. Watson, N., and Janota, M.S., **"Turbocharging the Internal Combustion Engine,"** Wiley Interscience, New York, 1982
15. Flaxington, D., and Szuzupak, D. T., **"Variable area radial-inflow turbine"**, 2nd Int. Conf. on Turbocharging and Turbochargers, Proc. of the IMechE, Paper C36/82, 1982
16. Franklin, P. C., and Walsham, B. E., **"Variable geometry turbochargers in the field"**, 3rd Int. Conf. on Turbocharging and Turbochargers, Proc. of the IMechE, paper C121/86, pp. 241-250, 1986
17. Kawaguchi, J., Adachi, K., Kono, S. and Kawakami, T., **'Development of VFT (Variable Flow Turbocharger),'** SAE Paper 1999-01-1242, 1999
18. Capobianco, M. and Gambarotta, A., **"Variable Geometry and Waste-Gated Automotive Turbochargers: Measurements and Comparison of Turbine Perforamance,"** J. of Eng. For Gas Turbines and Power, Vol 114, p.p. 553-560, July 1992

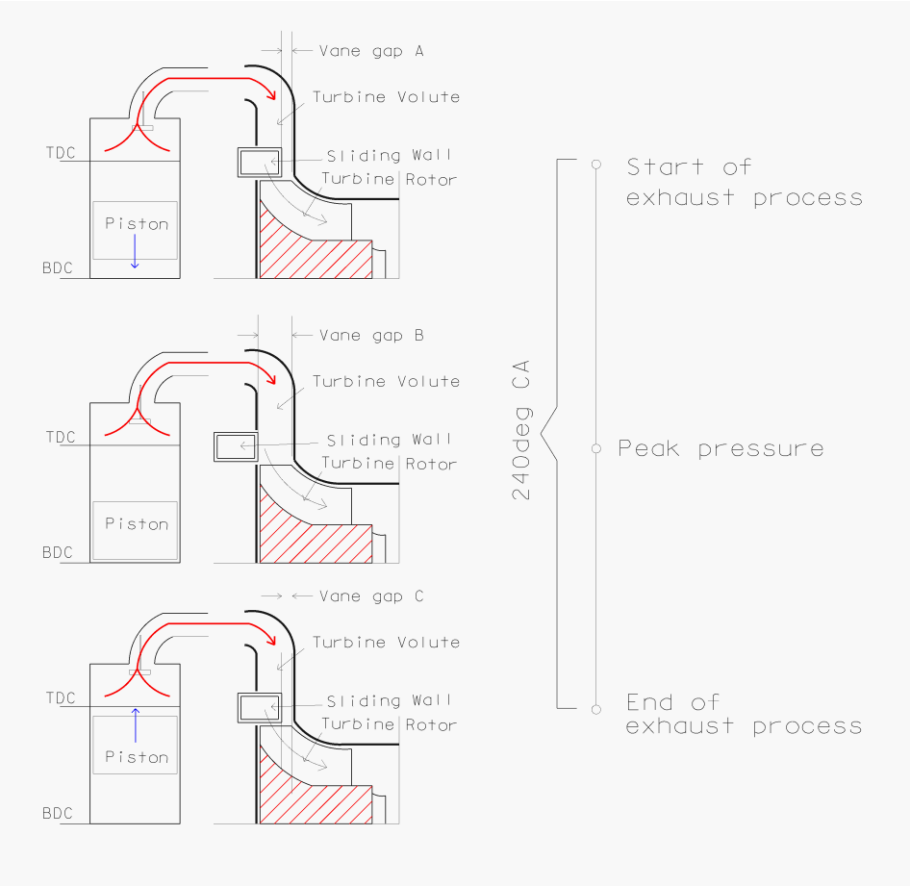


**Fig 1: VGT active control concept. Exhaust process cycle (240º CA) for one cylinder, where sliding vane gap A starts off in the closed (minimum gap) position at the start of the exhaust process, and progressively opens to the maximum gap (fully open) position B at peak pressure and then closes back to the minimum vane gap position C at the end of the exhaust process.**

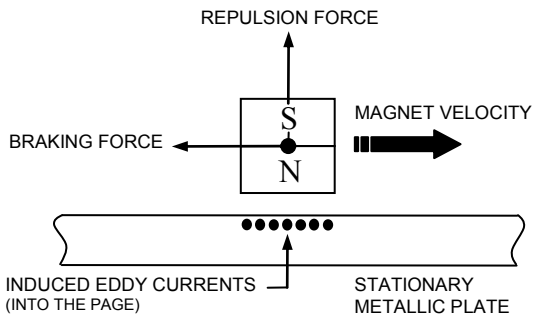


**Figure 2: Eddy-current Principle**

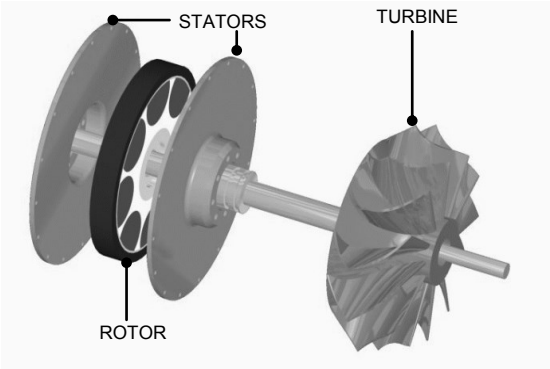


**Figure 3: Main components**

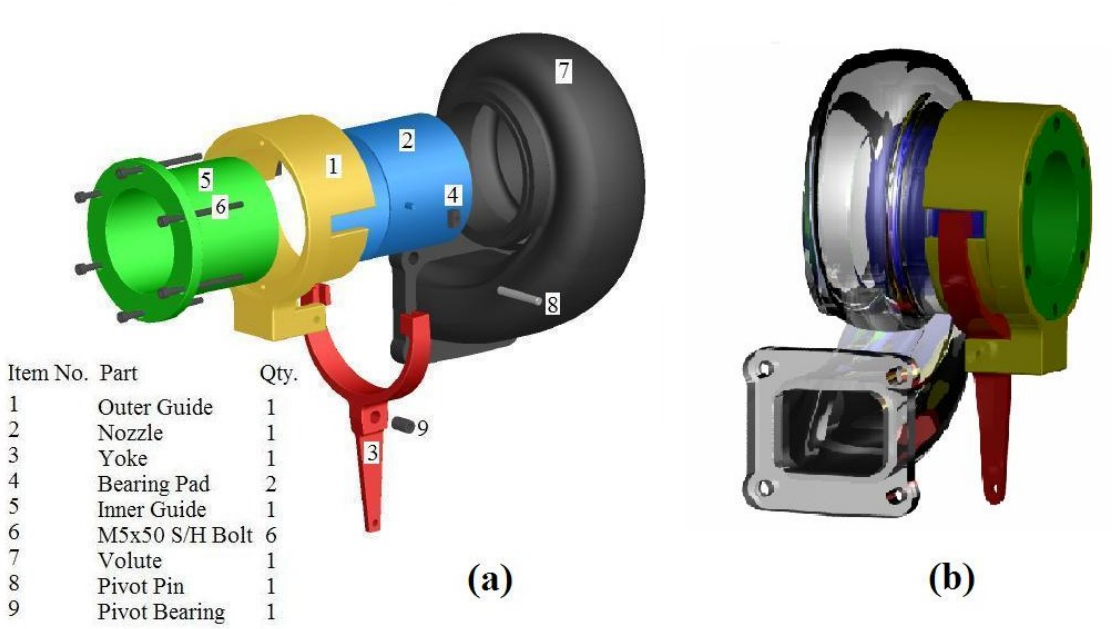


| Item No. | Part | Qty. |
|---|---|---|
| 1 | Outer Guide | 1 |
| 2 | Nozzle | 1 |
| 3 | Yoke | 1 |
| 4 | Bearing Pad | 2 |
| 5 | Inner Guide | 1 |
| 6 | M5x50 S/H Bolt | 6 |
| 7 | Volute | 1 |
| 8 | Pivot Pin | 1 |
| 9 | Pivot Bearing | 1 |

**Fig.4: (a) Active control turbocharger exploded view and (b) assembled turbocharger**

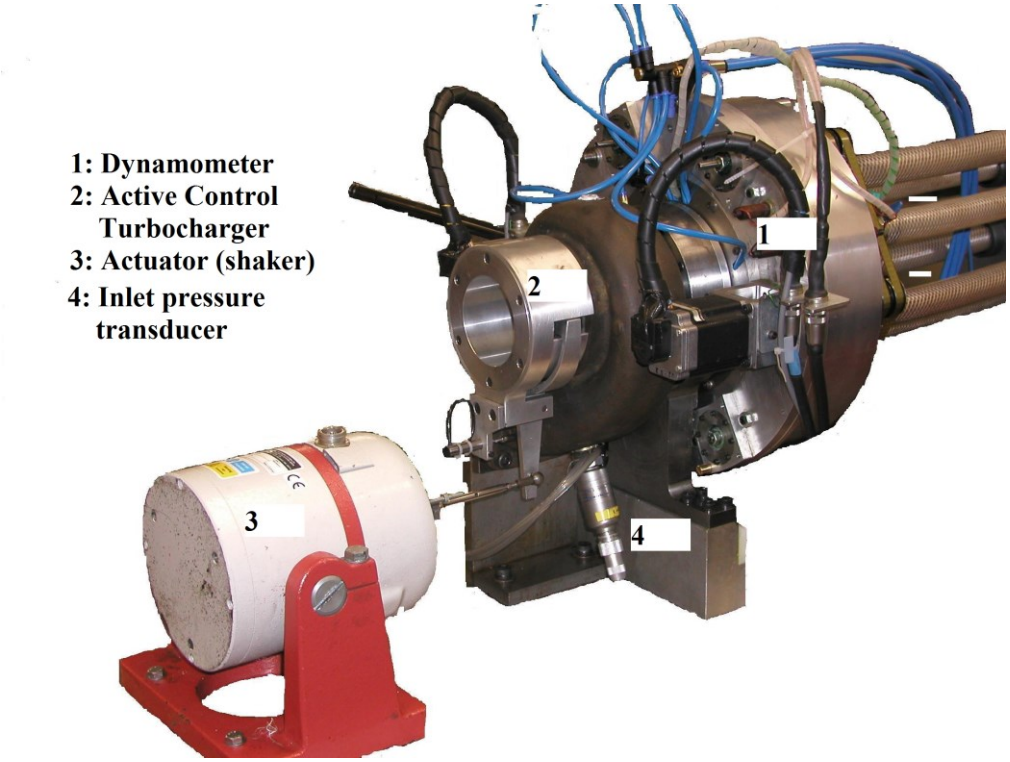


**Fig.5: Active control turbocharger with electrodynamic shaker and dynamometer.**

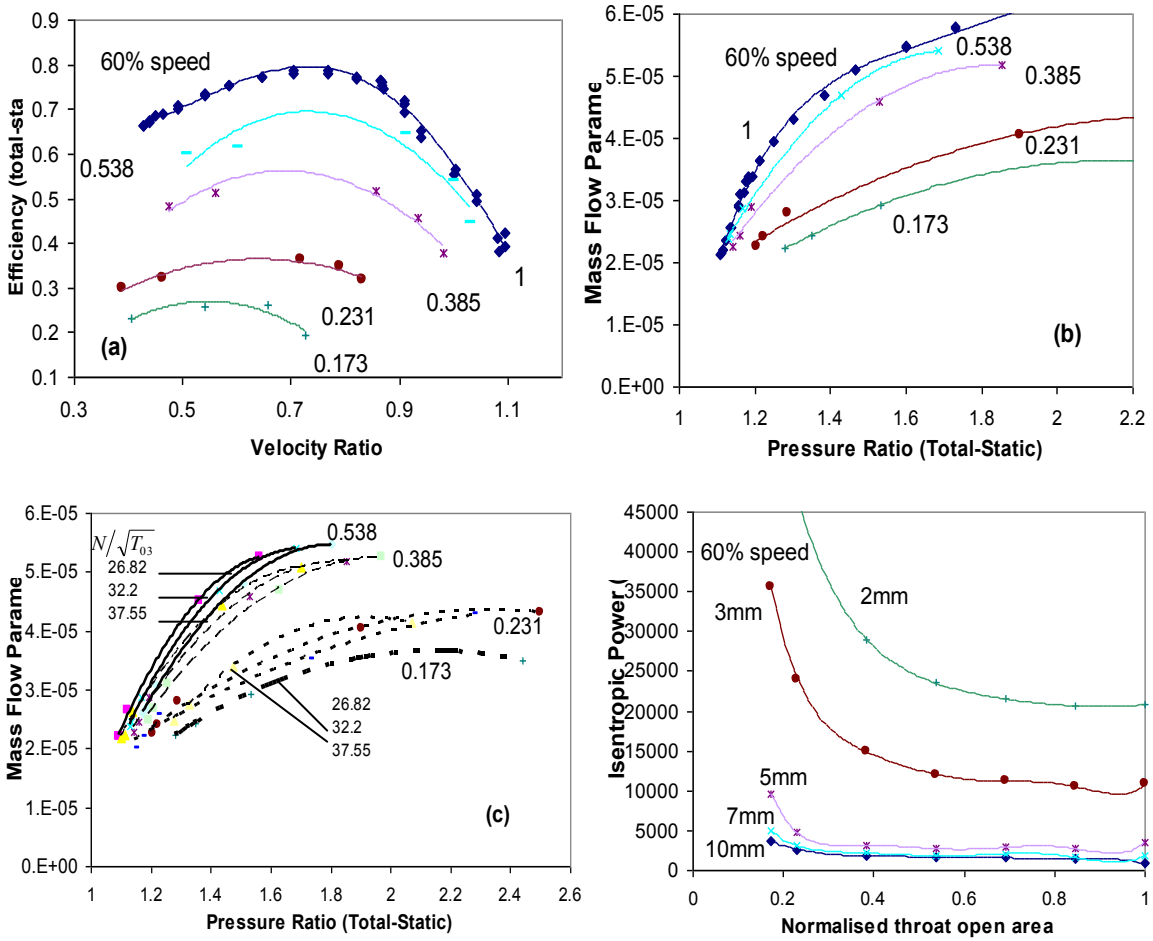


**Fig.6: (a) and (b) Steady state turbine maps for 60% equivalent speed and (c) overall VGT turbine map.**




**Fig.7: Isentropic power with throat are restriction for constant load lines (in mm dynamometer gap).**

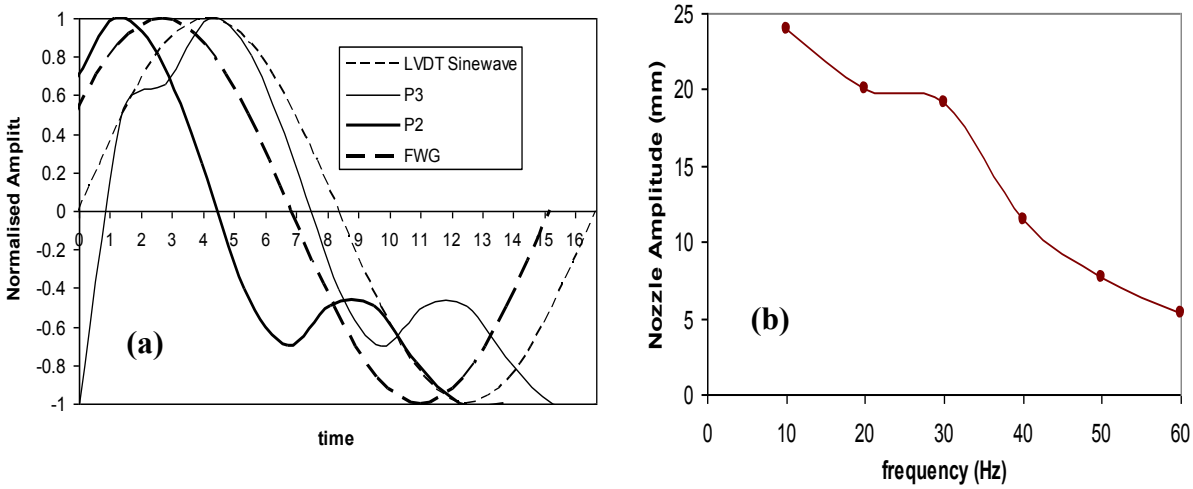


**Fig.8: (a) Available nozzle amplitude performance over (b) the test frequency range.**